SUPPLEMENT MATERIAL

1. Material and Methods

Vessel Isolation, Cannulation and Study

Excised cremaster muscles were placed in a cooled (-2° C) dissection chamber containing physiological saline solution (PSS) containing (in mmol/l) 145 NaCl, 4.7 KCl, 2 $CaCl_2$, 1 $MgSO_4$, 1.2 NaH_2Po_4, 4 glucose, 2 pyruvate. With the aid of a stereomicroscope (Olympus SZX12, Melville, NY), segments of 1A arterioles were microdissected. The vessel segment was transferred to a clear Lucite chamber filled with PSS, then each end of the vessel segment was cannulated with a glass micropipette (tip diameter approximately 80 μm) and secured with nylon mono-filament suture (11-0, Alcon, Ft. Worth, TX). The vessel and tubing were filled with PSS containing 1% albumin. The chamber was then transferred to the stage of an inverted microscope (model IX71, Olympus) coupled to a video camera (model TMC-7DSP, Pulnix, Glostrup, Denmark), electronic video caliper (Texas A&M, College Station, TX), and a data acquisition system (Powerlab, AD Instruments, Colorado Springs, CO) that allowed continuous measurement of internal diameter. The micropipettes were connected to independent reservoirs for control of luminal pressure by adjustment of reservoir height. Temperature of the bath was continuously monitored and maintained at 34° C by constant flow through the water jacket surrounding the vessel bath. A peristaltic pump (model Sci-Q 400, Watson Marlow, Wilmington, MA) was used for superfusion of the vessel with PSS at a rate of 3-5 ml/min. Arterioles were initially held at a pressure of 40 mmHg, then the pressure raised to 70 mmHg to induce spontaneous myogenic tone. To be considered viable, arterioles had to be free of pressure leaks, exhibit spontaneous tone, and reactive to agonists. Functionality of the vessels was

tested by myogenic responsiveness and dilation to the endothelium-dependent vasodilator, acetylcholine (1 μM).

Cerebral and mesenteric vessels were prepared in a similar fashion with the exception that superfusion buffers were maintained at 37°C.

Experimental Protocols:

Sample Preparation:

Vessels were isolated, mounted on glass cannula and checked for leaks as above. Vessels were then pressurized to 70 mmHg and lengthened to remove lateral bowing. For fixation 2% paraformaldehyde was added to the bath (20 minutes at room temperature). Vessels were subsequently permeabilized with 0.1% Tween 20 for 1 hour and then washed with a physiological salt solution.

Antibody labeling:

Elastin: Primary antibody used was rabbit anti-rat elastin polyclonal antibody (Chemicon International) supplied as a stock concentration of 1 mg/ml. For immunostaining the antibody was used at a final concentration of 10 μg/ml and applied abluminally for approximately 12 hr, at 4°C. Goat anti rabbit IgG, Alexa fluor 488 – conjugated antibody (10 μg/ml) was subsequently used to visualize primary antibody binding. The secondary antibody was applied abluminally for 1 hr at room temperature. Vessels were maintained at an intraluminal pressure of 70 mmHg during the labeling procedure.

Collagen: Primary antibody used was a rabbit anti-Rat Collagen Type 1 polyclonal antibody (Millipore) supplied as a stock concentration of 1 mg/ml. For immunostaining the antibody

was used at a final concentration of 1 μg/ml and applied abluminally for approximately 12 hr, at 4°C. Secondary antibody, goat anti-rabbit IgG, Alexa fluor 488 (final concentration 20 μg/ml) was applied abluminally for 1 hr at room temperature. As above, vessels were maintained at an intraluminal pressure of 70 mmHg.

Indicator labeling:

Alexa 633 Hydrazide: Vessels were incubated at room temperature in Alexa 633 hydrazide (0.2 μM; Molecular Probes) for 20 minutes. The hydrazide was prepared in physiological salt solution. After washing, staining was visualized by excitation at 633 nm (HeNe laser) at emission wavelengths of 650-750 nm.

4'6-diamino-2-Phenylindol (DAPI): DAPI (500 ng/ml) was applied abluminally for 20 mins at room temperature. DAPI was prepared in physiological salt solution. After washing, staining was visualized by excitation at 350 nm (using 2 Photon laser at 700 nm) at emission wavelengths of 400- 450 nm. DAPI nuclear stain was used only when tri-labeling (Alexa 633 hydrazide, specific elastin antibody; and nuclear localization) was performed to avoid spectral overlap with the secondary antibody. In other situations nuclei were labeled with Yo-Pro-1 iodide.

Yo-Pro-1 Iodide: Yo-Pro-1 Iodide (1 μL/ml; Molecular Probes) was applied abluminally for 20 minutes at room temperature. The indicator was prepared as a stock (1 mM) in physiological salt solution). After washing, staining was visualized by excitation at 488 nm (Argon laser) at emission wavelengths of 500 – 550 nm.

Dicarboxyfluorescein: DCF was prepared in Krebs buffer at a final concentration of 100 μM. DCF. Prior to vessel cannulation, one pipette tip was filled with DCF. For imaging, the DCF was advanced into the arterial lumen while additional DCF solution was added to the vessel superfusate. Image acquisition was then performed with the dye remaining in the lumen and the bath. Excitation was at 488 nm and emission was set from 500 - 600 nm. As DCF diffused into gaps between the cells, digital image inversion using Imaris software resulted in a shadow image of the VSMC which was then pseudo-colorized (Martinez-Lemus et al., FASEB J., 2004; Supplementary Information Figure I).

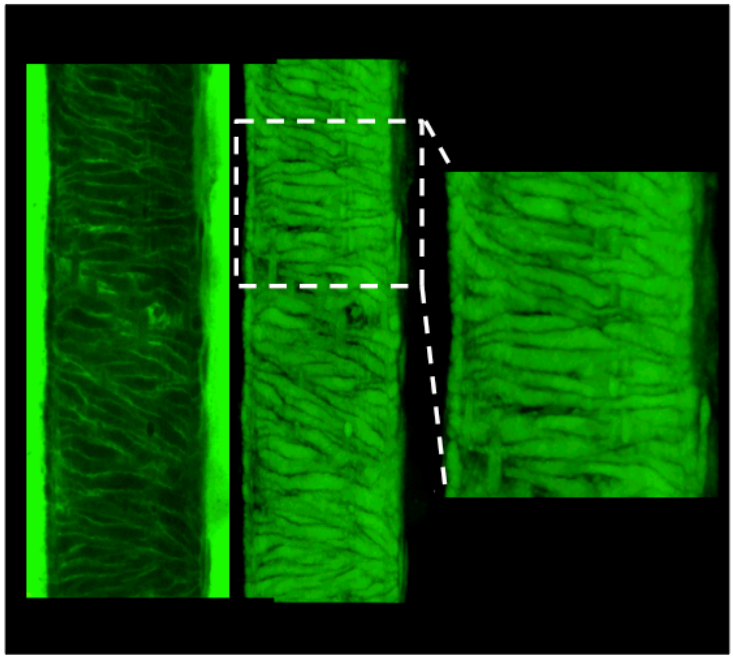

Supplementary Figure I: Left hand image shows a cannulated cremaster arteriole exposed to cell-impermeable DCF. The middle image shows the same image digitally inverted to provide the 'shadow image' of the VSMCs that has been pseudo-colored. The right hand image shows an enlarged area of vessel image as would be used for measurements of cell width and number of cells per unit length.

Imaging Parameters:

Spatial: For routine studies, image resolution was set at 512 x 512 pixels with image dimensions of 246 x 246 μm. Line scans were averaged over 3 lines with no additional requirement for frame averaging. Additional higher resolution images were collected at 1024 x 1024 pixels.

Temporal: Laser illumination was scanned at 400 Hz

Z-stack: Stack depths were typically taken over 30- 40 μm with step sizes of 0.05 - 0.3 μm.

Laser Power: Typical laser power levels employed were HeNe, 10%; Argon, 10-20%; and multiphoton, 50%

Objective : 60x water immersion lens, NA: 1.2

Microscope: Leica TCS-SP5

Image Processing

Image analysis was performed using Image J. Image stacks were independently saved according to the wavelength at which they were acquired. Depending on dual- or tri-labeling, individual stacks were merged on an image and pixel basis to obtain a composite stack. The composite was reduced to 256 colors and saved as an 8-bit avi file. The 3D viewer macro was used to visualize the composite stack both as a 3D rotating image and specific image planes. The orientation and axis of the blood vessel was adjusted to view the different layers of arterioles. In order to selectively visualize the EEL or IEL, images corresponding to those sections of the stack were summed on a pixel-to-pixel basis to obtain enhanced fluorescence signals and contrast of the structures.

Antibody Specificity and Autofluorescence

To demonstrate specificity of the staining procedure controls were performed where fixation, permeabilization and exposure to secondary antibody were performed in the absence of primary antibody. No staining resembling elastin fibers or collagen was evident in the absence of the primary antibody (Supplementary Figure II). Non-specific staining appeared limited to the outer vessel layer presumably reflecting binding to tissue damaged during vessel dissection (Supplementary Figure II).

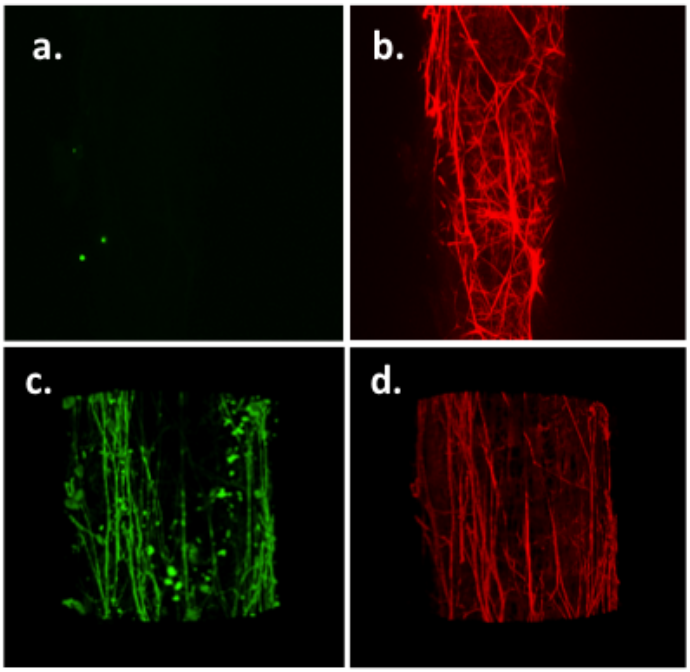

Supplementary Figure II: Demonstration of elastin antibody specificity. Panel a. secondary antibody (goat anti-rabbit IgG, Alexa fluor 488) alone; Panel b. corresponding Alexa 633 hydrazide staining; Panel c. staining with primary elastin antibody; and Panel d. corresponding Alexa 633 hydrazide staining

As autofluorescence approaches can be used for the imaging of elastin and collagen control studies were undertaken to determine any contribution of autofluorescence to our imaging data. To perform these studies permeabilized and fixed vessels were imaged in the absence of staining procedures. Laser power was initially set at levels used for the specific staining protocols (488 nm, 60 - 80 μW; 633 nm, 13-20 μW) after which illumination was increased to high levels (488 nm, 530-560 μW; 633 nm, 520-560 μW). At the laser powers routinely used in our studies no evidence of an autofluorescence component to images was detected (Supplementary Table I). Even at high laser powers only low-level autofluorescence signals were observed under the imaging conditions used (Supplementary Table I). In addition no bleed-through autofluorescence was detected between channels.

Supplementary Table I

Excitation Wavelength	Low Laser Intensity	High Laser Intensity
488	No signal	+
633	No signal	No signal
488 and 633	No signal	+

2. Results

Acute Effects of Collagenase on Cannulated Arterioles

Exposure of cannulated arterioles to type II collagenase (30 units/ml) for 5 min resulted in a 34.1 ± 4.0% increase in diameter which was reversed after washing (**Supplementary Figure IIIa**). In contrast, a similar treatment with elastase (0.05 U/ml; 5 mins) did not cause vasodilation

(**Supplementary Figure III**). Results are expressed as mean ± SEM of absolute vessel diameter (μm) (n = 13 for collagenase and 16 for elastase). Collagenase treatment caused an upward shift in the passive pressure-diameter relationship (**Supplementary Figure IIIb**) differing from the leftward shift caused by elastase (see Figure 2d main manuscript).

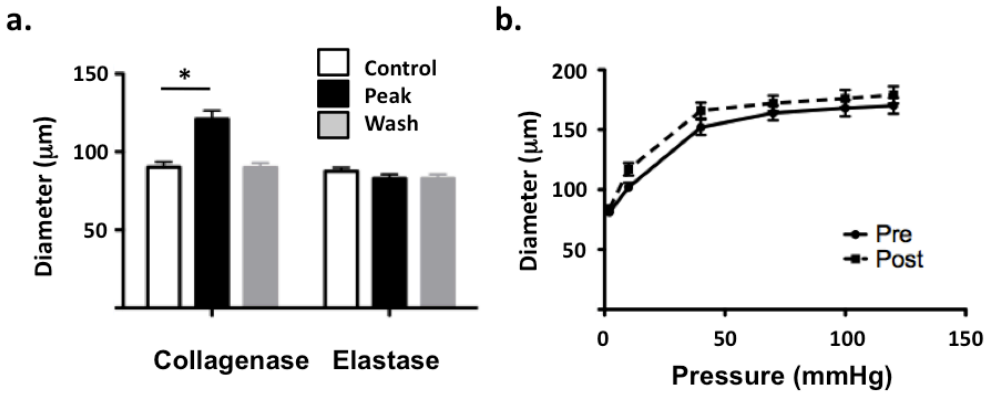

Supplementary Figure III: Panel a. - collagenase treatment caused dilation of myogenically active cremaster arterioles (n = 6). This effect was reversed by washing and is assumed to reflect the exposure of matricryptic sites or the generation of soluble vasoactive factors (see Davis G.E. et al., Am. J. Pathol. 156:1489-98, 2000). The effect of collagenase was in contrast to the effect of elastase which caused irreversible lengthening of the cannulated vessel segments. Panel b. – collagenase causes an upward shift in the passive pressure – diameter curve for cremaster arterioles (n = 6). This again contrasts with the actions of elastase that caused a leftward shift in the relationship, particularly evident at low pressures.

View of the Adventitial, Intimal and IEL Surfaces of Alexa 633 Hydrazide Stained Vessels

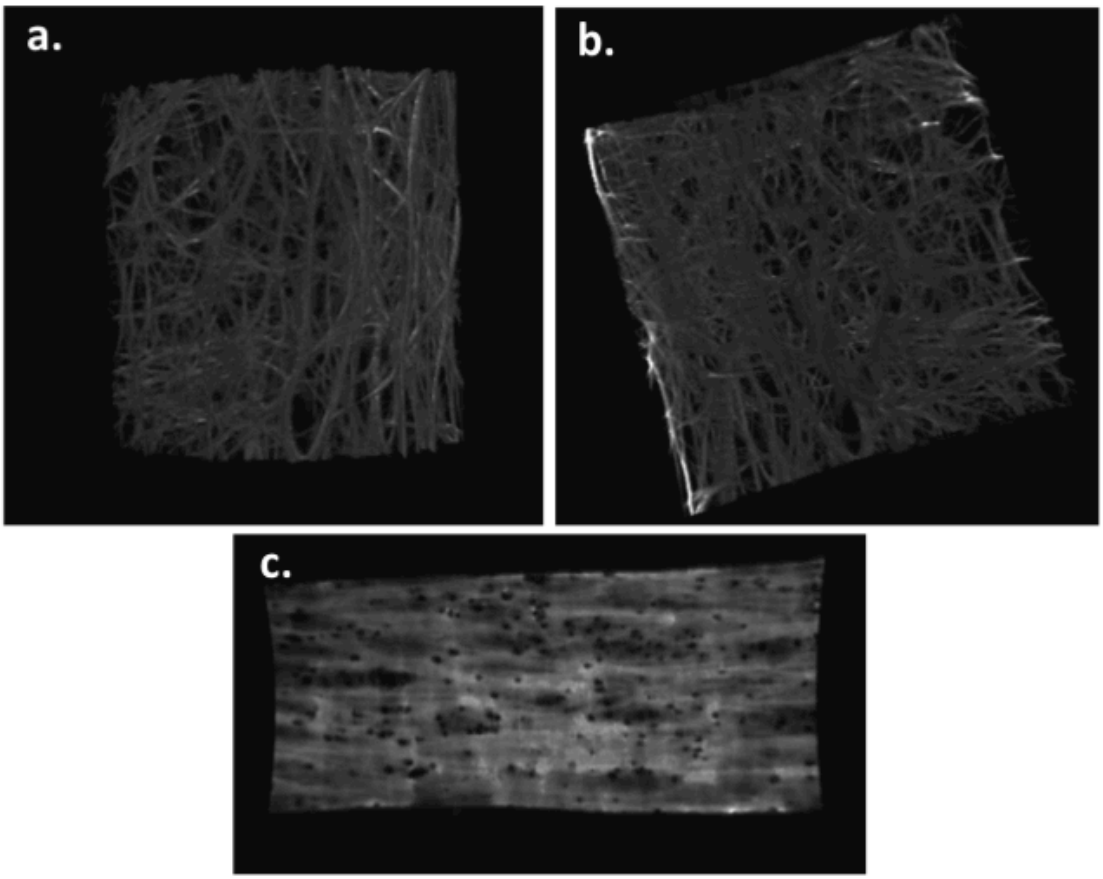

Supplementary Figure IV: Images of arterial wall illustrating Alexa 633 hydrazide staining of specific structural elements. Panel A shows the fibers (elastin) as viewed from the adventitial surface and B from the intimal view. Both images are from the same cremaster muscle arteriole. Panel C shows the IEL of a small cerebral artery. For each vessel, Z-dimension image slices were collected at a step thickness of 0.05 um.

Distribution of Type 1 Collagen in the Arteriolar Wall

Cremaster 1As were cannulated and pressurized as in the earlier studies. Vessels were fixed, permeabilized and incubated with an anti-type 1 collagen antibody followed by a FITC-labeled anti-rabbit IgG secondary antibody. Nuclei were stained with DAPI and advential/elastic fibers with Alexa-633. Type 1 collagen staining appeared more diffuse and restricted to the outer surfaces of the vessel. Importantly, the pattern of staining was distinct to the discrete fibers stained by either the Alexa-633 dye (**Supplementary Figure V**) or the specific elastin antibody (Figure 4, main manuscript).

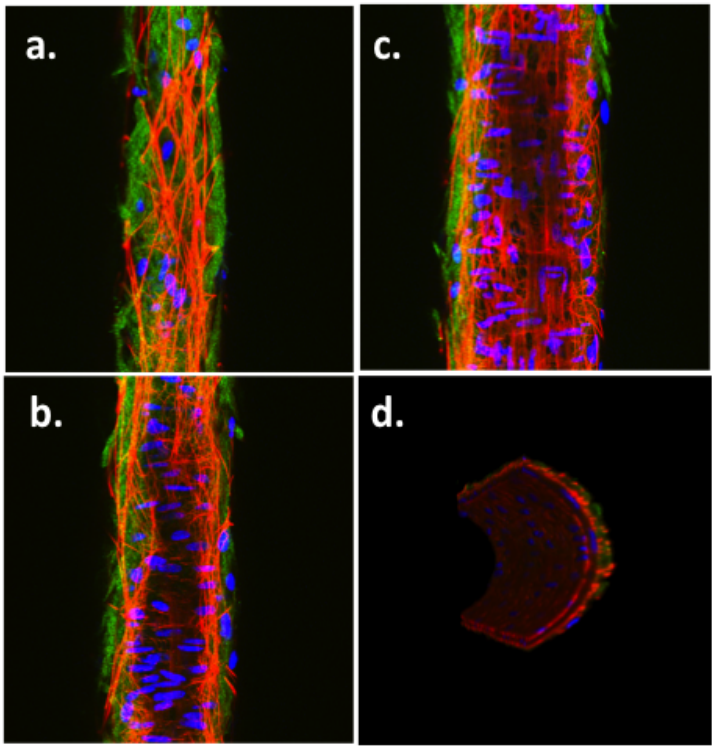

Supplementary Figure V: Staining of Type 1 collagen (green) in a cremaster arteriole shows a pattern distinct from the Alexa 633 hydrazide staining elastin-containing fibers. Panels a, b and c show differing optical planes through the vessel wall while Panel D shows an end-on view (see main manuscript for section details).

Biochemical Indices of Vessel Wall Heterogeneity Between Cremaster and Cerebral Vasculatures.

Given the apparent differences in the structure of the vessel wall between the cremasteric and mesenteric arteries versus those from the cerebral circulation it was expected that the latter vessels may show a higher ratio of muscle (as reflected by α actin content) to total protein. α actin content was determined using Western blotting and densitometry and expressed relative to total protein content. Total protein was measured using the BCA assay (Pierce, Thermoscientific Fisher, Rockford, IL). The amount of muscle protein in cremaster 1A and small cerebral and mesenteric arteries was expressed as arbitrary actin densitometry units per μg protein. Data were then expressed relative to the results obtained for cremaster 1A samples on a given Western blot. A significantly ($p < 0.05$) higher ratio was observed in small cerebral arteries (2.43 ± 0.52; $n = 5$) compared to either cremaster (1.0 ± 0.19; $n = 5$) or mesenteric (1.23 ± 0.11; $n = 5$) vessels (**Supplementary Figure VIa**). These data further support heterogeneity of the vascular wall between vascular beds but do not give direct insight into specific proteins.

Although a major component of elastin expression has been shown to occur during development (Mecham 2008) real time PCR was used to examine differences in the levels of mRNA for elastin in cremaster, mesenteric and cerebral vessels (as used in the imaging studies). PCR was performed using an Eppendorf Realplex cycler and SYBR green interchelation. Equal amounts of total vessel RNA extract (Melt Total Nucleic Acid isolation system, Ambion) were reverse-transcribed into cDNA using a Superscript III First-Strand synthesis system, (Invitrogen) according to the manufacturer's instructions. Sequence

specific primers for rat elastin (accession no. NM_012722) and rat β-actin (accession no. NM_031144) as a house keeping gene were designed as follows:

Elastin (forward): 5'-TTCTCCTATCTACCCAGGTGG-3'; and

(reverse): 5'-AAGATCACTTTCTCTTCCGG-3',

β-actin (forward): 5'-CCTCTATGCCAACACAGTGCTGTCT-3'; and

(reverse): 5'-GCTCAGGAGGAGCAATGATCTTGA-3'.

Samples (n=4) were performed in triplicate and each run included a no template and no enzyme control to test for contamination of assay reagents. To verify that only specific product was amplified, a melting point analysis was performed after the final cycle. Data were collected using Realplex software (Eppendorf) and relative quantification was performed using the comparative threshold (Ct) method after determining the Ct values for reference (β-actin) and the target gene, elastin, in each sample sets according to the $2^{-\Delta\Delta Ct}$ method (Livak and Schmittgen, 2001).

As shown in **Supplementary Figure VIb** mRNA levels for elastin were significantly ($p < 0.05$) lower in cerebral arteries compared to either cremaster or mesenteric vessels.

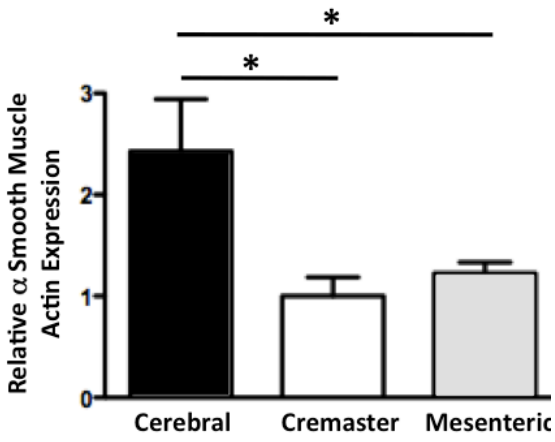

Supplementary Figure VIa: α-actin:total protein ratios for cerebral arteries, cremaster 1A and small mesenteric arteries. Results are expressed as arbitrary actin densitometry units per μg protein and are shown as mean ± SEM, n = 5.

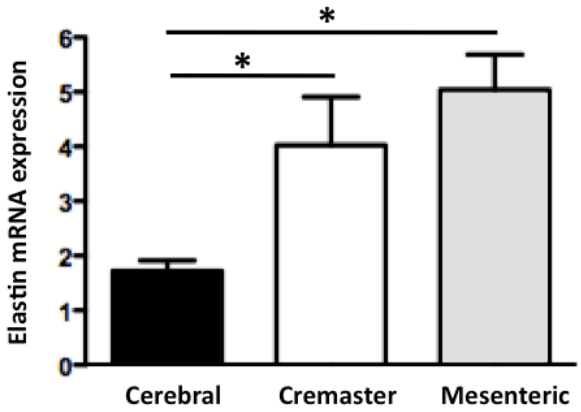

Supplementary Figure VIb: Elastin mRNA as measured by quantitative PCR. Results are expressed relative to β-actin as a housekeeping gene and are shown as mean ± SEM, n = 4. Similar results were obtained using an alternate housekeeping gene (GAPDH; data not shown).

Supplementary Movie Files

1. Rotating volume rendered 3D projection of a cannulated cremaster muscle 1A. The image has been reconstructed from a 3D image series with z sections taken at an interval of 0.3 μm. The playback speed of the movie is adjusted to 10 frames/sec

2. Movie file showing the individual images of the cremaster 1A used to produce the 3D image in Supplementary Movie File 1. The image stack begins at the adventitial surface

and progresses through to the intima. Alexa 633 hydrazide was used to stain the adventitial matrix fibers (elastin-containing; red) while the nuclei (green) were stained with Yo-Pro-1.

3. Rotating 3D image of a cannulated cerebral small artery. The image has been reconstructed from a 3D image series with z sections taken at an interval of 0.3 μm.

4. Movie file showing the individual images of the cerebral artery used to produce the 3D image in Supplementary Movie File 3. The image stack begins at the adventitial surface and progresses through to the intima. Alexa 633 hydrazide was used to stain the adventitial matrix fibers (elastin-containing; red) while the nuclei (green) were stained with Yo-Pro-1.

5. Rotating 3D image of a third order mesenteric artery. The image has been reconstructed from a 3D image series with z sections taken at an interval of 0.3 μm.

6. Movie file showing the individual images of the third order mesenteric artery used to produce the 3D image in Supplementary Movie File 1. The image stack begins at the adventitial surface and progresses through to the intima. Alexa 633 hydrazide was used to stain the adventitial matrix fibers (elastin-containing; red) while the nuclei (green) were stained with Yo-Pro-1.